
ELSEVIER Applied Mathematics and Computation 105 (1999) 195–210

APPLIED MATHEMATICS AND COMPUTATION

www.elsevier.nl/locate/amc

Advances in the implementation of the box-counting method of fractal dimension estimation

K. Foroutan-pour, P. Dutilleul *, D.L. Smith

Department of Plant Science, McGill University, Macdonald Campus, 21111 Lakeshore Road, Ste-Anne-de-Bellevue, Que., Canada H9X 3V9

Abstract

The box-counting analysis is an appropriate method of fractal dimension estimation for images with or without self-similarity. However, this technique, including processing of the image and definition of the range of box sizes, requires a proper implementation to be effective in practice. The objectives of this study were thus (1) to determine how to prepare an image for box-counting analysis; (2) to define reasonable preferences for using the Fractal Dimension Calculator software; and (3) to develop a routine procedure for defining the most appropriate range of box sizes for any one-piece image. Four fractal images were chosen for this study: the Koch curve, Koch coastline, Koch boxes, and Cross-tree. Our results show that the skeletons provide better material for the box-counting method since only lines and/or curves are responsible for the fractal dimension value. In the procedure of box counting for fractal dimension estimation, the image must be surrounded by a four-square frame with the least possible area and the condition of linear relationship must be satisfied in a log–log plot. Fractal dimension is to be estimated over the minimum number of boxes covering the image for each box size, after superimposing a reasonable number of grid offsets. In many cases, 25% of the shorter image side may provide an appropriate value for largest box size. However, for noisy or dispersed patterns, a smaller box size than this is needed. In the log–log plot with 12 box sizes, some points corresponding to smaller box sizes deviate from the straight line from a certain point on. The box size corresponding to this breakpoint will provide an appropriate smallest box size. The exercise of determining the most appropriate range of box sizes must be performed repeatedly for every individual image.

* Corresponding author. E-mail: cydp@musica.mcgill.ca.

0096-3003/99/$ – see front matter
PII: S0096-3003(98)10096-6

Keywords: Box counting; Fractal dimension estimation; Fractal images; Fractals; Image processing; Image skeletons; Smallest and largest box sizes

1. Introduction

1.1. Fractal geometry

Among the major recent achievements in understanding of structural disorder and its formation are fractal concepts [1]. A "fractal" designates a rough or fragmented geometric shape that can be subdivided into parts, each of which is (at least approximately) a reduced-size copy of the whole. Contrary to classical geometry, fractals are not regular and may have a non-integer dimension. Fractals are generally self-similar and independent of scale. Nature conforms to fractals much more than it does to classical shapes (spheres, cones, cylinders, etc.), and hence fractals can serve as models for many natural phenomena. Various natural shapes, such as sea coasts, mountains and rivers, have been described mathematically by fractal geometry [1–4]. Application of fractal theory allows description of various states of fragmenting and branching in biological, ecological and other systems [5–13]. Fractal concepts have provided a new approach for quantifying the geometry of complex or noisy shapes and objects. Fractal geometry has been proven capable of quantifying irregular patterns, such as tortuous lines, crumpled surfaces and intricate shapes, and estimating the ruggedness of systems [1].

1.2. Linear and non-linear fractals

Linear fractal images are the outcome of absolute generating processes and the information related to each step of the process can be calculated exactly [2,14]. For instance, in a linear fractal image like Koch boxes (Fig. 1(a)), seven new segments, three times smaller than the previous segment, are generated at each step in the generating process. Therefore, an exact mathematical calculation procedure follows. After the first step, the image contains seven ($N(s)$) segments whose size (s) is 1/3 that of the initial value; after the second step, the image contains 49 segments of size 1/9; and so on (Table 1). A straight line with a slope of 1.7712 can be perfectly fitted by plotting $\log(N(s))$ versus $\log(1/s)$ (Fig. 1(b)). In linear fractals, even after two steps of the generating process, the fractal dimension can be calculated exactly.

In non-linear fractal images, because of the existence of random elements there is a statistical (i.e., not deterministically mathematical) generating process and the information available at each step of the generating process is not exact

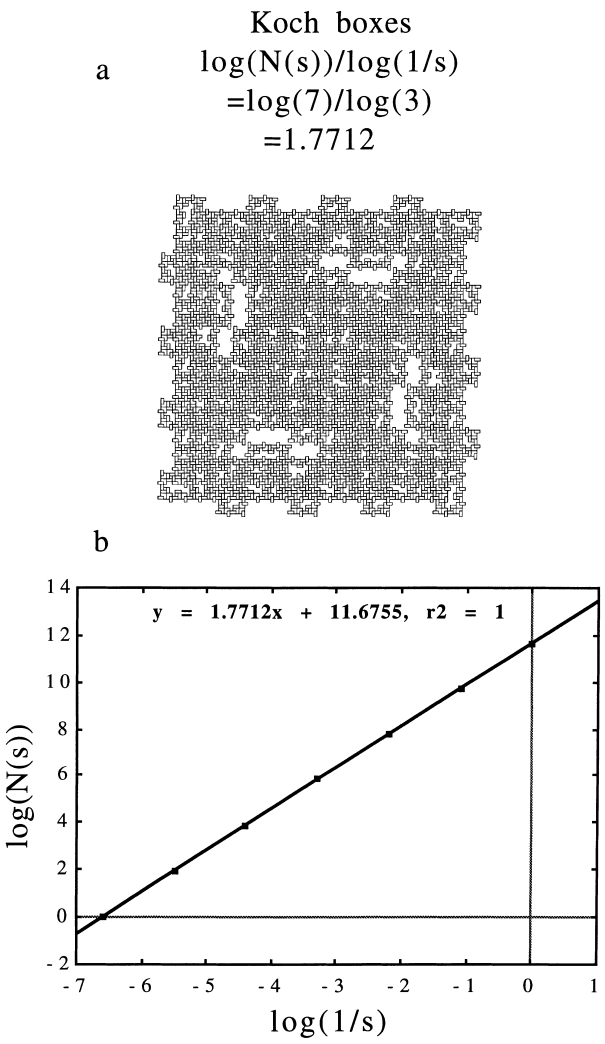

Fig. 1. (a) The Koch boxes image and (b) the plot of $\log(N(s))$ versus $\log(1/s)$ in direct relation to the generating process of the image.

[2,14]. Natural fractals fall into this category of fractals. For this reason, an appropriate method is needed to estimate the fractal dimension of non-linear images. Among a number of techniques discussed by Mandelbrot [1], the box-counting method was found to be the most desirable and appropriate method of fractal dimension estimation. In particular, the box-counting method is applicable to both linear and non-linear fractal images.

Table 1
Progressively transforming process into the final fractal pattern and the corresponding data points in the log–log plot for the Koch boxes image (Fig. 1)

s	$N(s)$	$\log(1/s)$	$\log(N(s))$
1	117649	0	11.6755
3	16807	−1.0986	9.7296
9	2401	−2.1972	7.7836
27	343	−3.2958	5.8377
81	49	−4.3944	3.8918
243	7	−5.4931	1.9459
729	1	−6.5917	0

1.3. Objectives of this study

In using the box-counting method, challenges arise when the range of box sizes is to be determined. In particular, defining the largest and smallest box sizes to use requires extreme care. In addition, the positioning of the grid to superimpose on the image has a critical effect on the resulting estimate of fractal dimension. Therefore, both factors should be verified [15–17].

Hereafter, we show how to process the image properly and assess the requirement of a linear relationship when plotting $\log(N(s))$ versus $\log(1/s)$ in order to estimate the fractal dimension with minimum error. Four images with known fractal dimension were used to validate our procedure. Obviously, two properties of an image, its size and structural details, may have a significant effect on the definition of the range of its box sizes. The objectives of this study were thus (1) to determine how to prepare an image for box-counting analysis; (2) to define reasonable preferences for using the Fractal Dimension Calculator software (this software was chosen for the grid offset option it provides); and (3) to develop a routine procedure for defining the most appropriate range of box sizes for any individual image.

2. Materials and methods

2.1. Scanning and image processing

Four fractal images with known fractal dimension were chosen for this study. These images are: the Koch curve, Koch coastline, Koch boxes and Cross-tree, with fractal dimension of 1.5, 1.2619, 1.7712 and 1.5850, respectively. The Cross-tree fractal image was created by adding two branches emerging from the middle point of the initial segment, which gave three branches, each of length 1/2, plus a stem. Thereafter, each of the three branches was submitted to the same generating process, each of them giving three

sub-branches of length 1/4, and so on. The Cross-tree fractal image used here is the result of six steps of the generating process. Its fractal dimension can be calculated on the basis of the production of branches whose size is one half the previous at each step ($\log 3/\log 2 = 1.5850$).

The chosen images were scanned at a resolution of 72 dpi (as required by the Fractal Dimension Calculator software) with an Adobe PhotoshopTm scanner AX-1200 for PowerPC Macintosh, version 3.0 (Nikon Scantouch Corporation, Electronic Imaging Engineering Division, Tokyo, Japan). Since the information contained in an image is defined not by the resolution, but by the number of pixels horizontally and vertically, we scanned the images in a sufficiently large manner. One of the advantages in using images of large size is the availability of a wider range of box sizes in the Fractal Dimension Calculator software, in order to increase the accuracy of fractal dimension estimation. Finally, the scanned images were saved as 8-bit grayscale PICT files.

Image processing was performed with NIH version 1.60, an image processing software developed to operate on Apple Macintosh computers and written by Wayne Rasband of the National Institutes of Health, Bethesda, Maryland. The software is in the public domain through the internet (http://rsb.info.nih.gov/nih-image). Each 8-bit grayscale PICT file was converted to 1-bit black and white, by using the threshold command. This conversion was followed by a "cropping" operation, which included the removal of unwanted parts of the image from the screen. Thereafter, the image skeletons were taken using the skeleton command. Finally, the images, including the original and skeletal forms, were saved as PICT files, as required by the Fractal Dimension Calculator software.

2.2. The box-counting method

A number of techniques that can be used for fractal dimension estimation were discussed by Mandelbrot [1]. In this study, the box-counting method was used because it is easy, automatically computable, and applicable for patterns with or without self-similarity [18]. In this method, each image is covered by a sequence of grids of descending sizes and for each of the grids, two values are recorded: the number of square boxes intersected by the image, $N(s)$, and the side length of the squares, s. The regression slope D of the straight line formed by plotting $\log(N(s))$ against $\log(1/s)$ indicates the degree of complexity, or fractal dimension, between 1 and 2 ($1 \leqslant D \leqslant 2$) [1]. An image having a fractal dimension of 1, or 2, is considered as completely differentiable, or very rough and irregular, respectively. The linear regression equation used to estimate the fractal dimension was

$$\log(N(s)) = \log(K) + D\log(1/s),$$

where K is a constant and $N(s)$ is proportional to $(1/s)^{-D}$ [1].

The box-counting method was operated using the Fractal Dimension Calculator software for the Apple Macintosh computer, written by Dr. Paul D. Bourke of the School of Architecture, University of Auckland, New Zealand (available from Paul Bourke at pdbourke@ccul.aukuni.ac.nz). By default, this software uses 12 box sizes. Optionally, the range of box sizes and the number of grid offsets can be controlled by users. Two important options are the range of box sizes and the number of grid offsets to be used. Obviously, the smallest and largest box sizes that fix the range of box sizes depend on the resolution of the scanned image, including its size and its structure. Defining the range of box sizes is thus a common problem for work with two-dimensional fractal images. As the strict estimation of a fractal dimension value requires the minimum box covering [19], using this option effectively improves the accuracy of fractal dimension estimation. An exhaustive search for minimum box covering is very time consuming, especially for images of large size. For this reason, a series of preliminary tests was performed over images with different sizes, and the results demonstrated that 100 was a reasonable number of grid offsets. Therefore, all our estimates of fractal dimension were obtained over the minimum number of boxes covering the image after 100 grid offsets unless fewer offsets were needed.

Regression analysis with two regression lines fitted simultaneously by using dummy variables was carried out by procedure GLM of SAS Version 6 [20]. The linear regression equation used for final estimation of the fractal dimension was fitted with SAS procedure REG [20].

3. Preamble

3.1. Two-dimensional images and determinants of fractal dimension

The value of the fractal dimension of an image is determined by various structural parameters. Generally, elements of nature appear physically as solid objects with a degree of roughness at their perimeter, as objects whose structures are built mainly by a branching network with a certain degree of ramification, at as objects having both structures.

As discussed by Corbit and Garbary [19], the value of the fractal dimension could be influenced by local and/or global aspects of structure. Roughness and smoothness of the edges of an object refer to local effects, whereas the number of times a given individual has branched is defined as a global effect.

From a geometric perspective, structural parameters affecting the value of the fractal dimension of an image whose details are continuously connected appear as lines and/or curves. Smaller lines indicate the degree of the ramifying process, and curves indicate the level of tortuousness of the perimeter or branches. Basically, lines and/or curves are the geometric elements which represent the complexity of an image and determine the value of the fractal dimension.

The only parameter that does not affect the real value of fractal dimension, but has an effect on the process of determining the most appropriate range of box sizes in the box-counting method, is the thickness of lines or curves. Thickness of lines or curves can affect the determination of the range of box sizes in two ways. First, images may have lines and/or curves with a thickness greater than the smallest possible box size available for box-counting analysis. Second, there may be a lack of uniformity in thickness for lines and curves over the image. In this study, all images were computer-generated with uniform thickness for all lines and curves, but in many practical situations, lack of uniformity in thickness may cause a serious problem. Thickness of lines and/or curves in an image has a major effect on the determination of the smaller box sizes. Because of the original thickness of lines and curves in an image and the changes resulting from the scanning operation on it, special attention must be paid to this parameter when determining the range of box sizes.

In order to prevent any difficulty caused by the thickness of lines or curves, images were skeletonized before determining the best range of box sizes. This provided images with uniform thickness of one pixel for any lines and curves, and removed any problem related to thickness of lines and curves. Some results for original images without skeletonizing will also be discussed.

4. Results and discussion

4.1. How to surround the image with a four-square frame

Using the box-counting method to estimate the fractal dimension of an image requires the image to be surrounded by a four-square frame (i.e., a square or a rectangle). The way an image is surrounded by a four-square frame affects the determination of the most appropriate range of box sizes when applying the box-counting method. The best way of surrounding an image with a four-square frame is by minimizing the area covered by the frame. The four-square frame surrounding the image has a major effect on determining the largest box size. For instance, having an image contained in a smaller four-square frame facilitates the fitting of a straight line in the log/log plot, by reducing the possible range of box sizes and providing closer box sizes (based on the use of 12 box sizes by default in the Fractal Dimension Calculator software).

Fig. 2 shows that an image can be surrounded by a four-square frame with the least possible area in two ways: by surrounding the image with the frame as close as possible to the image's details (Fig. 2(a)) or by turning an image a bit to the left or to the right in order to achieve minimum covering (Fig. 2(b)), compared to alternatives (Figs. 2(c) and 2(d)).

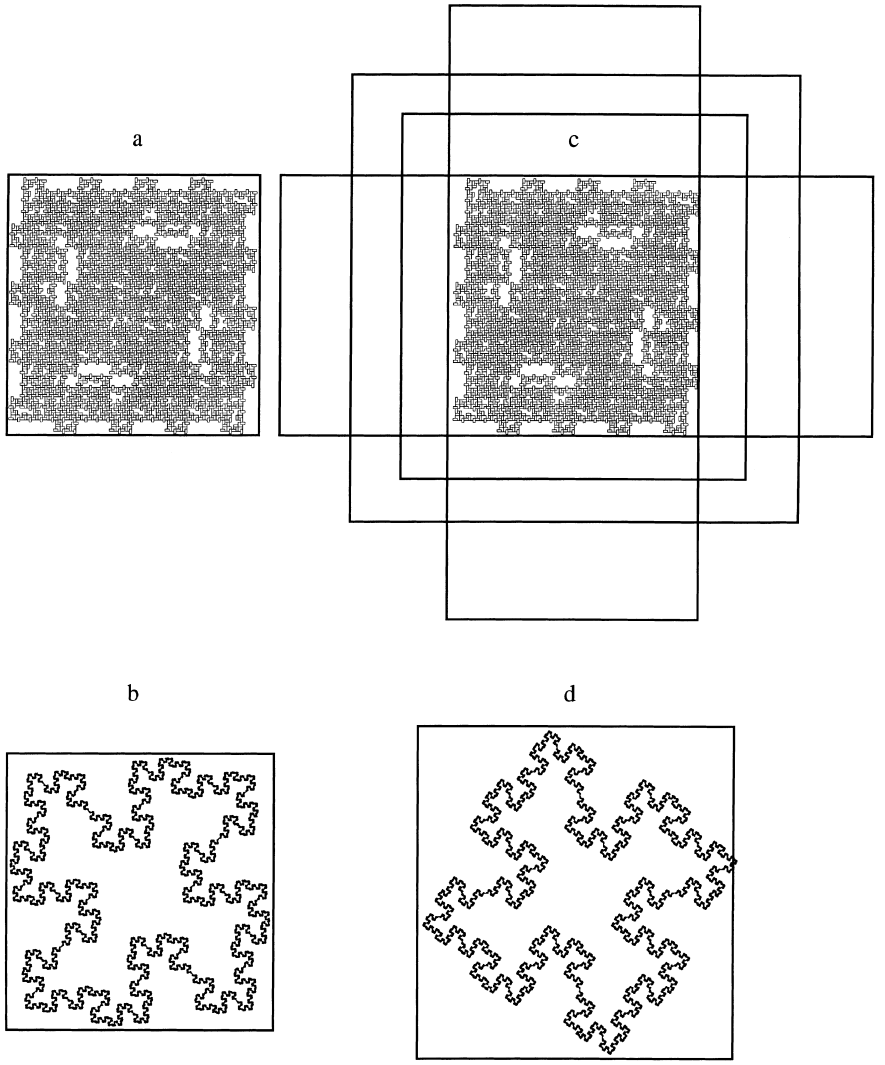

Fig. 2. Two effective ways for surrounding an image by a four-square frame (a and b), compared to alternatives (c and d).

4.2. Determining the largest box size

Images can be surrounded by a square or a rectangle, depending on the length of the image's sides. For images that are surrounded by a rectangle, the division of box sizes is based on the length of the shorter side of the image. Practically, the largest size to be considered in the range of box sizes could be

the shorter side of the image. However, a preliminary study showed that any box size greater than 25% of the shorter side of the image, chosen as largest size in the range of box sizes, led to very poor information (results not reported). Such a choice increased the risk of error in many cases, which confirms previous studies [15–17]. Therefore, in our study, 25% of the shorter side of the image was chosen as a starting point for the largest box size.

This choice is suitable for many but not all images. For images which are very noisy or whose structure is such that almost all the area inside the four-square frame surrounding the image is occupied by structural details, this size may not be a good choice. For large box sizes even smaller than 25% of the shorter side of the image, images with noisy or dispersed structures may appear as solid objects because they intersect almost all the boxes of the grid. This will cause serious problems of bias for the box-counting method which will then overestimate the value of the fractal dimension. Table 2 shows results of the box-counting method for several large box sizes equal to or smaller than 25% of the shorter image side of the Koch boxes image. This image is noisy, with details appearing in all of the area of the square frame surrounding it. As our results indicate it, when all of the boxes in the grids are intersected by the image, regression coefficients are very close to 2, which represent the image as a solid object. As boxes are descending in size and grids with smaller box sizes are covering the image, regression coefficients decrease and grids begin to capture the information.

Fig. 3(a) shows the regression line corresponding to Table 2. These results confirm that the largest box size cannot be a size providing the box-counting method with misleading information, by representing the image as a solid object. Our analysis of the Koch boxes image showed that the box size that led

Table 2
Results of the box-counting method for an increasing number of large box sizes, starting with 25% or less of the shorter side of the image (bottom of the table) for the Koch boxes image

s	$N(s)$	$\log(1/s)$	$\log(N(s))$	Regression coefficient [a]
31	5160	−3.4340	8.5487	1.9264
33	4596	−3.4965	8.4329	1.9277
34	4336	−3.5264	8.3747	1.9289
36	3870	−3.5835	8.2610	1.9313
38	3524	−3.6376	8.1674	1.9374
77	926	−4.3438	6.8309	1.9538
154	245	−5.0370	5.5013	1.9730
307	64	−5.7268	4.1589	2.0000
614	16	−6.4200	2.7726	–

[a] The coefficient of the regression of $\log(N(s))$ on $\log(1/s)$ was calculated as points corresponding to box sizes less than 25% of the shorter side of the image were added (from bottom to top of the column). For example, the regression coefficient of 2.0 corresponds to the straight line fitted for two box sizes, including 25% and 12.5% of the shorter side of the image.

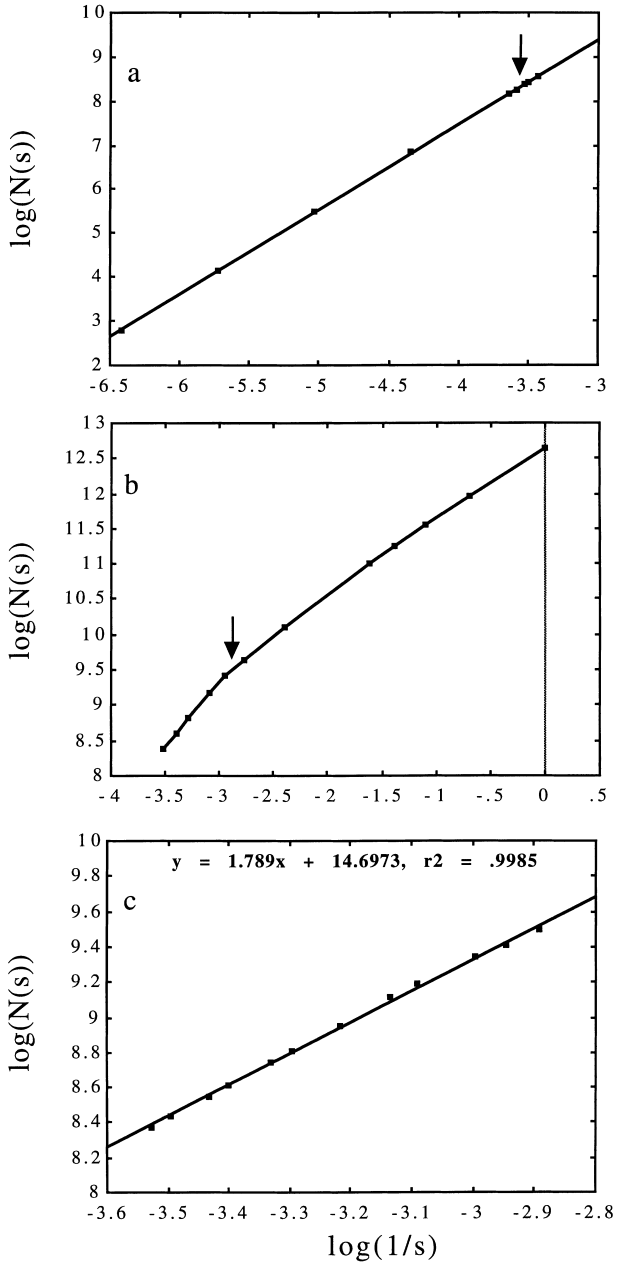

Fig. 3. Plot of $\log(N(s))$ versus $\log(1/s)$ for determining (a) the largest box size, (b) the smallest box size, and (c) the final estimation of fractal dimension for the Koch boxes image.

to the intersection of approximately 85% of the boxes by the image could be used as largest box size. This size is indicated by an arrow in Fig. 3(a).

Overall, there is no point having box sizes greater than 25% of the shorter side of the image. In many cases, 25% of the shorter side of the image will provide an appropriate value for largest box size. However, for noisy or dispersed patterns, a smaller box size than this may be needed, as indicated by our analysis of the Koch boxes image.

4.3. Determining the smallest box size

To determine the most appropriate value for smallest box size, a series of 12 box sizes was considered, starting with the largest box size found in the procedure explained above, followed by sequential divisions of this size by powers of two, and finishing with sizes of one to five pixels. This type of range of box sizes will provide information over a wide range of scales. In addition, this range of scales will determine the box sizes for which the requirement of a linear relationship in the log–log plot is met, or not.

Fig. 3(b) shows the plot of $\log(N(s))$ versus $\log(1/s)$, based on the 12 box sizes considered. This graph clearly indicates that some of the points corresponding to the smaller box sizes (i.e., larger $\log(1/s)$ values) deviate from the straight line fitted, with the largest box size (i.e., smallest $\log(1/s)$ value) as origin. Deviation from a straight line can thus be expected to lead to an underestimation of the fractal dimension value for the skeleton of an image.

For a certain box size, geometric elements of the image, which are lines and/or curves, appear as individual parts, each of which is almost covered by one box in the grid. From this box size to the smallest box size (one pixel) which corresponds to the largest $\log(1/s)$ value, the $N(s)$ value is just measuring the lines of the object. For this reason, the slope of the regression line over these points in the log–log plot will be close to 1. Generally, deviation from linearity demonstrates that from a certain resolution, the information provided does not incorporate the real complexity of the image. This is why these points must be eliminated from the range of box sizes to be used for analysis. Therefore, the smallest box size in the range of box sizes to work with will correspond to the last point or breakpoint for which a straight line can be approximately fitted in the first part of the log–log plot.

4.4. Determination of breakpoint in the log–log plot

We considered two procedures to verify the breakpoint between points used to fit a straight line in the first part of the log–log plot and the rest of the points in the plot. The first procedure consists in fitting a regression line over all

points and then eliminating points one by one, starting from the smallest box size to the largest box size, until a regression line to which almost all points are attached is obtained. The last point on this regression line will be the break-point that defines the best smallest size for the range of box sizes. In this procedure, more sizes may sometimes be needed. For instance, using this procedure for the data of Fig. 3(b), a few more box sizes between the 5th and 6th were indicated since the regression lines fitted to the first five and first six points were attaching almost all the points, with little deviation for the first six points (results not shown).

Another procedure that we considered is based on dummy variables used in a regression analysis with two regression lines [21]. This procedure provided identical results for the data of Fig. 3(b). Since it is expected that the log–log plot cannot satisfy two straight lines for some images, this procedure must be applied with caution.

4.5. Final estimation of the fractal dimension

After finding the largest and smallest box sizes, the range of box sizes is determined. To estimate the value of the fractal dimension for the Koch boxes image, the box-counting method was performed with 12 new box sizes, including the largest and smallest sizes found above. Fig. 3(c) displays the plot of $\log(N(s))$ versus $\log(1/s)$. The regression model shows that the estimated value of the fractal dimension is 1.7890, which approximates the expected value of 1.7712 very closely.

We applied the same procedure to estimate the fractal dimension of the three other images. Fig. 4 shows the images and their expected and estimated fractal dimensions.

4.6. Results for original, unskeletonized images

To show the typical effect of thickness of lines and curves on the outcome of the box-counting method of fractal dimension estimation, the original images were analyzed without skeletonizing. With this exception, the procedure developed above was followed. After determining the largest box size, 12 box sizes were defined as in Fig. 3(b). The $\log(N(s))$ versus $\log(1/s)$ plot shown in Fig. 5(a) corresponds to the Koch curve image displayed in Fig. 4(a). It appears that from a certain point (see the arrow), the curve deviates from a straight line. This deviation represents an overestimation, contrary to the image skeletons for which an underestimation was observed. The reason is that after a certain point, box sizes are smaller than the line width and the $N(s)$ value then just measures the area of a solid object [16,17,22]. To estimate the

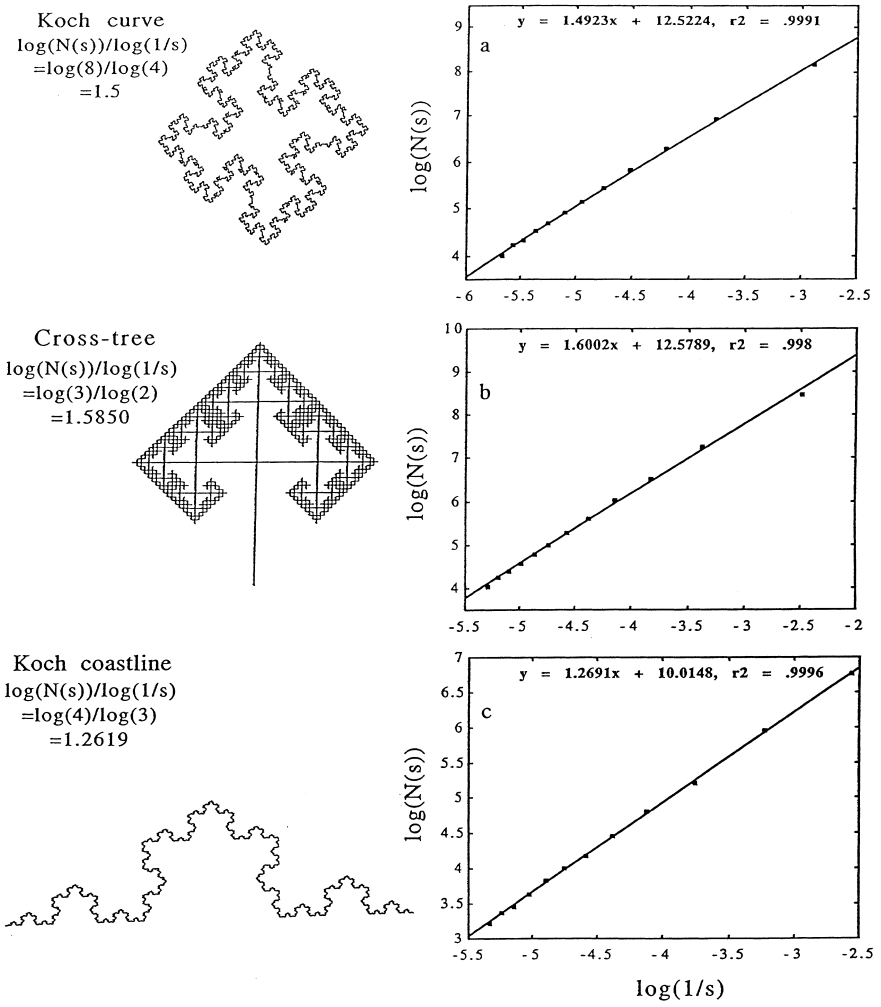

Fig. 4. Koch curve (top), Koch coastline (bottom) and Cross-tree (middle) images, and the corresponding plot of $\log(N(s))$ versus $\log(1/s)$ for final estimation of their fractal dimension.

fractal dimension, points deviating from the straight line were eliminated and new box sizes between the smallest and the largest were defined. Fig. 5(b) shows the log–log plot and the estimated value of fractal dimension for the Koch curve image. The estimated fractal dimension is 1.5866, whereas the expected fractal dimension is 1.5. The difference between expected and estimated fractal dimensions indicates the interference of line and curve thickness with the outcome of the box-counting method for unskeletonized images.

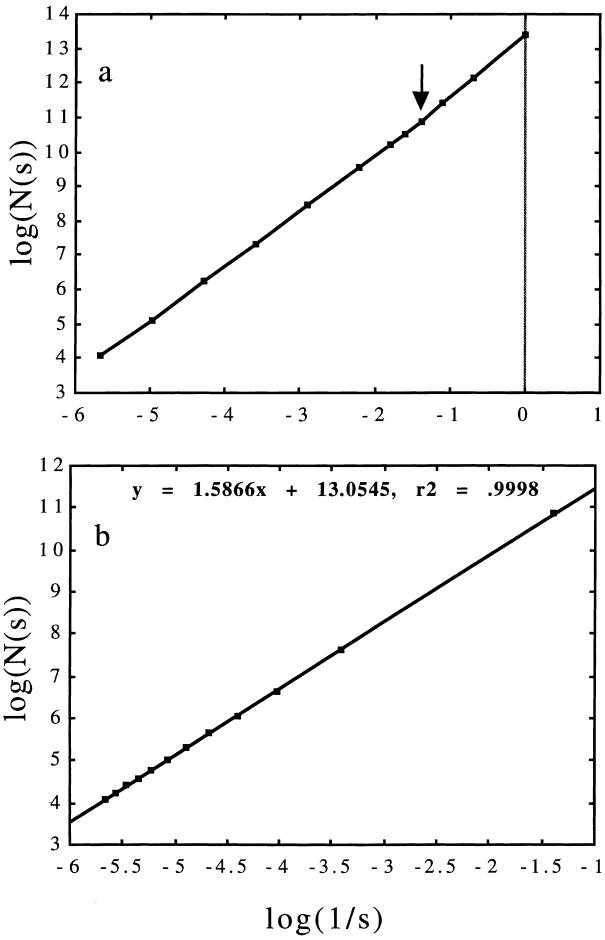

Fig. 5. Plot of $\log(N(s))$ versus $\log(1/s)$ for (a) the process of determining the smallest box size and (b) the final estimation of fractal dimension for the Koch curve image.

4.7. Comparison of fractal dimension estimates for skeletonized and unskeletonized images

With the exception of the previous section, all our results were obtained with skeletonizing of the images. Our results show that more accurate estimation of fractal dimension can be obtained by applying the box-counting method to skeletal images. The reason for that lies mainly in the effect of line and curve thickness on the determination of the range of box sizes. The plot of $\log(N(s))$ versus $\log(1/s)$ shows sharper deviation from the straight line with a more recognizable breakpoint for the skeleton, whereas the deviation is slight and

the breakpoint is hard to capture for the original image. The thickness of lines and curves may affect even the larger box sizes, resulting in further reduced accuracy in the estimation. Unfortunately, this problem cannot be controlled. It must be noted that the problem caused by thickness of more than one pixel (smallest possible box size) for lines and curves will be worse in practice for images representing the branching pattern of real objects because of non-uniform thickness overall. Our study demonstrates that skeletal images are likely to provide better material to estimate the value of fractal dimension by using the box-counting method.

5. Conclusions

In two-dimensional images, since only lines and/or curves are responsible for the value of the fractal dimension, the image skeletons provide better material for the box-counting method. However, extreme care must be taken in the choice of the range of box sizes for the analysis. In estimating the fractal dimension by using the box-counting method, the image must be surrounded with a four-square frame with the least possible area and the condition of a linear relationship must be satisfied in a log–log plot. The fractal dimension is to be estimated over the minimum number of boxes covering the image for each box size, after superimposing a reasonable number of grid offsets. In particular, operating a high number of grid offsets for larger box sizes is very necessary. In many cases, 25% of the shorter side of the image will provide an appropriate value for largest box size. However, for noisy or dispersed patterns, a smaller box size than this is needed. For large box sizes less than 25% of the shorter side of the image, images with noisy or dispersed structures may appear as solid objects because they intersect almost all the boxes of the grid. Fitting a straight line over a series of 12 box sizes (starting with the largest box size found, followed by sequential divisions of this by powers of two, and finishing with sizes of one to five pixels), with the largest box size as origin, indicates that from a certain point on, points corresponding to smaller box sizes deviate from the straight line. The box size corresponding to that breakpoint will provide an appropriate smallest box size. Determining the most appropriate range of box sizes is a common problem for any image and the exercise must be performed repeatedly for every individual image.

References

[1] B.B. Mandelbrot, The Fractal Geometry of Nature, Freeman, New York, 1983.
[2] S. Frontier, Application of fractal theory to ecology, in: P. Legendre, L. Legendre (Eds.), Developments in Numerical Ecology, NATO Scientific Affairs Division, New York, 1987.

[3] B.B. Mandelbrot, Fractal geometry: What is it, and what does it do? in: F.R.S. Fleischmann, D. Tildesley, R.C. Ball (Eds.), Fractals in the Natural Sciences, Princeton University Press, Princeton, NJ, 1989.
[4] M. Schroeder, Fractals, Chaos, Power Laws, Freeman, New York, 1991.
[5] F.P. Agterberg, Fractals, multifractals, and change of support, in: R. Dimitrakopoulos (Ed.), Geostatistics for the Next Century, Kluwer Academic Publishers, Boston, 1994.
[6] P.A. Burrough, Fractal dimensions of landscapes and other environmental data, Nature 294 (1981) 240–242.
[7] D.L. Critten, Fractal dimension relationships and values associated with certain plant canopies, J. Agric. Engng. Res. 67 (1997) 61–72.
[8] F. He, P. Legendre, C. Bellehumeur, J.V. Lafrankie, Diversity pattern and spatial scale: A study of a tropical rain forest of Malaysia, Environ. Ecol. Stat. 1 (1994) 265–286.
[9] B.T. Milne, Measuring the fractal geometry of landscapes, Appl. Math. Comput. 27 (1988) 67–79.
[10] K.L. Nielsen, P.L. Jonathan, H.N. Weiss, Fractal geometry of bean root systems: Correlations between spatial and fractal dimension, Am. J. Bot. 84 (1997) 26–33.
[11] R.D. Otto, An evaluation of forest landscape spatial pattern and wildlife community structure, For. Ecol. Manage. 89 (1996) 139–147.
[12] C.E. Puente, A fractal-multifractal approach to geostatistics, in: R. Dimitrakopoulos (Ed.), Geostatistics for the Next Century, Kluwer Academic Publishers, Boston, 1994.
[13] B.J. West, A.L. Goldberger, Physiology in fractal dimensions, Am. Sci. 75 (1987) 354–365.
[14] H.E. Stanley, Fractals and multifractals: The interplay of physics and geometry, in: A. Bunde, S. Havlin (Eds.), Fractals and Disorded Systems, Springer, New York, 1991.
[15] B.H. Kaye, A Random Walk through Fractal Dimensions, Weinheim, New York, 1994.
[16] J. Soddell, R. Seviour, A comparison of methods for determining the fractal dimensions of colonies of filamentous bacteria, Binary 6 (1994a) 21–31.
[17] J. Soddell, R. Seviour, Using box counting techniques for measuring shape of colonies of filamentous micro-organisms, in: R.J. Stonier, X.H. Yu (Eds.), Complex Systems: Mechanism of Adaptation, IOS Press, Amsterdam, 1994b.
[18] H.O. Peitgen, H. Jurgens, D. Saupe, Chaos and Fractals New Frontiers of Science, Springer, New York, 1992.
[19] J.D. Corbit, D.J. Garbary, Fractal dimension as a quantitative measure of complexity in plant development, Proc. R. Soc. Lond. B 262 (1995) 1–6.
[20] SAS Institute Inc., SAS User's Guide: Statistics, Version 6. SAS Institute Inc., Cary, NC, 1989.
[21] N.R. Draper, H. Smith, Applied Regression Analysis, Wiley, New York, 1981.
[22] P. Bourke, Fractal dimension calculator user manual (available from Paul Bourke at pdbourke@ccul.aukuni.ac.nz), 1993.